

# Peptide Binding to Lipid Bilayers. Binding Isotherms and $\zeta$ -Potential of a Cyclic Somatostatin Analogue<sup>†</sup>

Georgi Beschiaschvili and Joachim Seelig\*

Department of Biophysical Chemistry, Biocenter of the University of Basel, Klingelbergstrasse 70, CH-4056 Basel, Switzerland

Received May 3, 1990; Revised Manuscript Received August 24, 1990

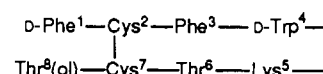
**ABSTRACT:** The binding of the cyclic somatostatin analogue SMS 201-995, (+)-D-Phe<sup>1</sup>-Cys<sup>2</sup>-Phe<sup>3</sup>-D-Trp<sup>4</sup>-(+)-Lys<sup>5</sup>-Thr<sup>6</sup>-Cys<sup>7</sup>-Thr(ol)<sup>8</sup>, to neutral and negatively charged lipids was investigated with a centrifugation assay and with electrophoretic and monolayer methods. Monolayers and bilayers were composed of 1-palmitoyl-2-oleoyl-*sn*-glycero-3-phosphocholine (POPC) and 1-palmitoyl-2-oleoyl-*sn*-glycero-3-phosphoglycerol (POPG), either in pure form or in a 75/25 (mol/mol) mixture. The expansion of monolayer films demonstrated the intercalation of the peptide between the lipid molecules with a surface area requirement of 135 Å<sup>2</sup> per peptide molecule, indicating a parallel alignment of the peptide long axis with the membrane surface. Above a limiting pressure of 32.5 mN/m for POPC and 38.5 mN/m for POPG, peptide penetration was no longer possible. The peptide binding isotherm could be measured for mixed POPC/POPG bilayers up to a peptide concentration of 0.5 mM. Due to electrostatic attraction, binding between the positively charged peptide and the negatively charged membrane surface was enhanced as compared to the binding to a neutral membrane. After correction for electrostatic effects by means of the Gouy-Chapman theory, the binding isotherm as well as the electrophoretic  $\zeta$ -potential measurement could be described by the same partition equilibrium with a surface partition constant of  $K_p = 36 \pm 4 \text{ M}^{-1}$  (at 0.1 M NaCl). About 60–70% of SMS 201-995 is probably embedded in the headgroup region with little penetration into the lipid core. The partition constant increases with increasing salt concentration or with decreasing lipid lateral pressure. The peptide effective charge seen by the membrane is  $z_p = 1.3$ , which is smaller than the nominal charge of  $z = 2$ .

The interaction of proteins with lipids involves both hydrophobic and electrostatic forces. For a simple partition equilibrium between water and a bulk hydrocarbon phase, the two forces are opposing each other: the hydrophobic effect drives the nonpolar residues into the oil phase, whereas the electrostatic interaction forces the charged amino acids into the aqueous phase. The hydrophobicity scale of amino acids, as derived from water-hydrocarbon partitioning studies (Nozaki & Tanford, 1971), has become a fundamental ingredient of modern protein folding theories [cf. Engelman et al. (1986)]. A simple partition equilibrium is, however, insufficient for membrane studies since it takes into account neither the complex molecular structure of the lipid interface nor the specific conformation of the interacting protein. The presence of electric dipoles and net electric charges at the membrane surface can enhance or weaken protein binding, and the penetration of the protein into the highly ordered hydration layer at the membrane surface may affect the hydrophobic entropy balance. Finally, an amphipathic helix with opposing polar and apolar faces will interact differently with the membrane than a related molecule where charged and hydrophobic amino acids are clustered at opposite ends of the helix.

The problem of protein-membrane interaction has been investigated intensely with simple, well-defined lipid-peptide model systems [cf. Surewicz and Epand (1984, 1985, 1986), Jacobs and White (1986, 1989), Jain et al. (1985), and Lee et al. (1989)]. Individual aspects of peptide and lipid structure were systematically varied and related to the corresponding changes in the binding parameters. The problems encountered in such studies are 2-fold. First, in order to obtain a meaningful binding isotherm the degree of binding,  $X_b$  (moles of

bound protein/mole of total lipid), should be known as a function of the free peptide concentration,  $c_{eq}$ , over as large a concentration range as possible, which is often difficult due to peptide aggregation, low peptide solubility, or micellization of membranes. In addition, technical limitations may not allow the direct measurement of  $X_b$ , but rather indirect parameters such as the light scattering intensity, the phase transition temperature, the formation of excimers, etc. are detected, and these are difficult to interpret in molecular terms. Second, the proper quantitative analysis of the binding isotherm requires models that consider separately electrostatic and hydrophobic effects. If the two are lumped together in a single binding constant the physical mechanisms of binding are obscured. A comparison of the binding properties of different peptides or different lipid systems is only meaningful if hydrophobic and electrostatic energy contributions can be considered separately.

We have addressed both questions in a binding study involving the cyclic peptide SMS 201-995 (charge +2)



in mixture with phosphatidylcholine/phosphatidylglycerol membranes. The octapeptide SMS 201-995 is an analogue of the hormone somatostatin but with greater biological activity (Maurer et al., 1982). Little is known about its interaction with membranes, but the possibility of a hydrophobic association mechanism is suggested by the presence of three aromatic amino acids near the N-terminal. A negative lipid component could further enhance peptide binding through electrostatic attraction. We have therefore measured the binding of SMS 201-995 to mixed phosphatidylcholine/phosphatidylglycerol (75/25 mol/mol) membranes by means of a centrifugation assay and have obtained the thermodynamic

\*Supported by the Swiss National Science Foundation Grant 31-27505.89.

binding isotherm. In addition, we have determined the electrophoretic mobility ( $\zeta$ -potential) under identical experimental conditions and have analyzed both the binding isotherm and the  $\zeta$ -potential by means of the Gouy-Chapman theory [cf. McLaughlin (1977, 1989)]. The combination of the two approaches considerably simplifies the quantitative analysis and allows a rather precise evaluation of the binding mechanism, the binding constant, and the effective charge of the peptide. As a third experimental approach we have measured the expansion of phospholipid monolayers due to peptide penetration. If performed at constant monolayer pressure, the area increase can be converted into a binding isotherm (Seelig, 1987). These expansion studies shed light on the peptide penetration power as a function of lipid packing.

## MATERIALS AND METHODS

**Materials.** SMS 201-995 was kindly provided by SANDOZ AG (Basel, Switzerland) and had a purity of better than 95%. The peptide concentration was determined with UV spectroscopy by using an absorption coefficient of  $\epsilon = 5700 \text{ M}^{-1} \text{ cm}^{-1}$  ( $\lambda = 280 \text{ nm}$ ) (Holladay et al., 1977). 1-Palmitoyl-2-oleoyl-*sn*-glycero-3-phosphocholine (POPC)<sup>1</sup> and 1-palmitoyl-2-oleoyl-*sn*-glycero-3-phosphoglycerol (POPG) were purchased from Avanti Polar Lipids (Birmingham, AL). Some binding experiments were also carried out with selectively deuterated POPC synthesized according to Tamm and Seelig (1983). These samples were used simultaneously for NMR measurements (Beschiaschvili & Seelig, 1990b).

**Binding Assay.** About 8–10 mg of lipid in the appropriate molar ratio POPC/POPG (75/25) was mixed in dichloromethane or chloroform and the solvent removed first in a stream of nitrogen and then under high vacuum. Two hundred microliters of buffer (either 0.1 M NaCl, 10 mM Tris-HCl, pH 7.4, or 0.154 M NaCl, 10 mM Tris-HCl, pH 7.4) containing the desired concentration of SMS 201-995 was added. The samples were vortexed for an extended period of time, followed by several freeze-thaw cycles and further vortexing to ensure a homogeneous equilibration of peptide. The suspension was centrifuged for 2 h at 120000g in an airfuge and the clear supernatant removed. The SMS 201-995 concentration in the supernatant was determined by UV spectroscopy ( $\lambda = 280 \text{ nm}$ ) after appropriate dilution. The molar amount of peptide bound per mole of total lipid, denoted  $X_b$  in the following, could then be calculated from the difference between the peptide concentration before and after equilibration with the lipid phase.

**Microelectrophoresis.** Multilamellar vesicles for  $\zeta$ -potential measurements were prepared by the method of Bangham et al. (1974). The POPC/POPG (75/25 mol/mol) mixture, typically 4 mg of total lipid, was dissolved in chloroform/methanol/water (20:9:1 v/v/v) [cf. Toner et al. (1988)] and the solvent removed by rotatory evaporation for at least 30 min, followed by at least 1 h under high vacuum. Five milliliters of buffer (100 mM NaCl, 10 mM Tris-HCl, pH 7.4) was added together with a few glass beads and the suspension was shaken gently. The desired amount of SMS 201-995 was added to the buffer after preparation of the vesicles. Electrokinetic mobilities were measured with a Rank Brothers Mark II microelectrophoresis apparatus, using a cylindrical cell and platinum electrodes. Care was taken to focus at the stationary layer.

<sup>1</sup> Abbreviations: PC, 1,2-diacyl-*sn*-glycero-3-phosphocholine; PG, 1,2-diacyl-*sn*-glycero-3-phosphoglycerol; POPC, 1-palmitoyl-2-oleoyl-*sn*-glycero-3-phosphocholine; POPG, 1-palmitoyl-2-oleoyl-*sn*-glycero-3-phosphoglycerol; NMR, nuclear magnetic resonance.

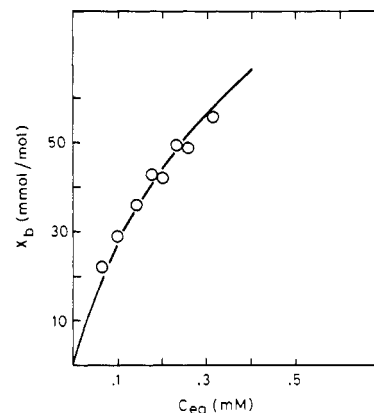


FIGURE 1: Binding of SMS 201-995 to phosphatidylcholine/phosphatidylglycerol (75/25 mol/mol) bilayer membranes. The amount of peptide bound per mole of total lipid is plotted versus the equilibrium concentration of peptide free in solution. The solid line is the theoretical binding curve calculated with a partition equilibrium ( $K_p = 36 \text{ M}^{-1}$ ) taking into account electrostatic effects by means of the Gouy-Chapman theory and also  $\text{Na}^+$  binding ( $K_{\text{Na}} = 0.6 \text{ M}^{-1}$ ) to PG (0.1 M NaCl, 10 mM Tris-HCl, pH 7.4, 20 °C).

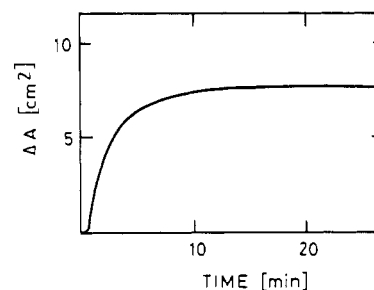


FIGURE 2: Area increase of a pure POPG monolayer compressed at 25 mN/m upon injection of a 6.5  $\mu\text{M}$  peptide solution (0.154 M NaCl, 10 mM Tris-HCl, pH 7.4). Total surface area was  $A = 48 \text{ cm}^2$ .

**Monolayer Measurements.** The monolayer apparatus consisted of a round Teflon trough designed by Fromherz (1975) with a total area of 322  $\text{cm}^2$ , divided into eight compartments (Type RMC 2-T, Mayer Feinttechnik, Göttingen, FRG). The surface pressure was measured by the Wilhelmy plate method using plates cut from filter paper (Whatman, No. 1). The interaction of SMS 201-995 with the lipid monolayer was studied at constant surface pressure and was evaluated from the increase in area of the monolayer due to penetration of peptide into the lipid [cf. Seelig (1987) and Seelig and Macdonald (1989)]. The buffer composition was 154 mM NaCl and 10 mM Tris-HCl, pH 7.4. The temperature was maintained at the 20 °C.

## RESULTS

**Peptide SMS 201-995 Binding to POPC/POPG Bilayers.** A centrifugation assay (cf. Materials and Methods) was used to measure the binding of the peptide to mixed POPC/POPG bilayers (75/25 mol/mol) in buffer (0.1 M NaCl, 10 mM Tris-HCl, pH 7.4). By freeze-thaw cycles and extensive vortexing a true chemical equilibrium was ensured. The change in the initial peptide concentration upon addition of lipid allowed the determination of bound peptide per total lipid,  $X_b$ . Figure 1 provides the experimental binding isotherm where  $X_b$  is plotted as a function of the peptide equilibrium concentration,  $C_{\text{eq}}$ . The solid line corresponds to the best fit to the data, calculated according to a partition equilibrium combined with the Gouy-Chapman theory as discussed below.

Binding data on the same membrane system were also obtained at a buffer composition of 0.154 M NaCl and 10 mM Tris-HCl, pH 7.4, and are included in Figure 4 in order to

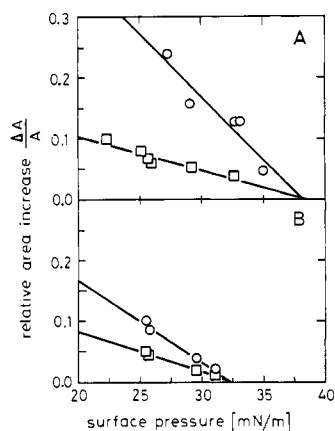


FIGURE 3: Relative area increase,  $\Delta A/A$ , of different monolayers upon injection of two different SMS 201-995 peptide solutions. (A) Pure POPG monolayers with peptide concentrations of  $1.3 \times 10^{-5}$  M (○) and  $3 \times 10^{-6}$  M (□). (B) Pure POPC monolayers with peptide concentrations of  $6 \times 10^{-5}$  M (○) and  $3 \times 10^{-5}$  M (□) (0.154 M NaCl, 10 mM Tris-HCl, pH 7.4).

allow a comparison with monolayer binding isotherms.

**Monolayer Binding Experiments.** The peptide SMS 201-995 intercalates between ordered lipids as can be demonstrated by monolayer experiments. In Figure 2 a lipid monolayer was formed with pure POPG on an aqueous subphase (0.154 M NaCl, 10 mM Tris-HCl, pH 7.4) and the lateral pressure was electronically adjusted to a constant value of  $\pi = 25$  mN/m. When the peptide was injected into the subphase, the monolayer area,  $A$ , increased and a stable equilibrium was reached after 5–10 min. The extent of peptide intercalation, measured as monolayer expansion  $\Delta A$ , depended on the packing density of the lipids and decreased with increasing monolayer pressure. Figure 3 summarizes the variation of the relative area increase,  $\Delta A/A$ , as a function of the monolayer pressure for pure POPG (Figure 3A) and pure POPC (Figure 3B) monolayers and for two different peptide concentrations.  $\Delta A/A$  decreased linearly with the monolayer lateral pressure  $\pi$ ; from the intersection of the straight lines with the  $\pi$ -axis a limiting pressure of  $38.5 \pm 0.5$  mN/m ( $32.5 \pm 0.5$  mN/m) for POPG (POPC) monolayers was derived. Above this pressure, the peptide can no longer penetrate into the monolayer. The cutoff pressure is independent of the peptide concentration but is influenced by the lipid composition. The higher cutoff pressure observed for pure POPG monolayers suggests that negatively charged lipids facilitate the association of the oppositely charged peptide with the membrane.<sup>2</sup> However, since the cutoff pressure for a given membrane system is independent of the peptide concentration, the differences between POPC and POPG cannot be explained by a simple electrostatic model (the sole role of electrostatic effects is to increase the interfacial concentration of peptide) but suggest a different structure of the two monolayer interfaces. Whether this difference is an exclusive property of the monolayers or is also carried over into the bilayer state is not known at present.

The expansion of the monolayer area,  $\Delta A$ , can be explained by the incorporation of  $n_p$  peptide molecules of area  $A_p$ . Since the pure lipid film (initial area  $A$ ) contains  $n_L$  lipid molecules of area  $A_L$ , the extent of peptide binding,  $X_b = n_p/n_L$ , can be calculated according to (Seelig, 1987)

$$X_b = n_p/n_L = (\Delta A/A)(A_L/A_p) \quad (1)$$

<sup>2</sup> Similar differences in the cut-off pressures have been observed for the binding of substance P, a positively charged neurotransmitter, to POPC and POPG monolayers (Seelig & Macdonald, 1989).

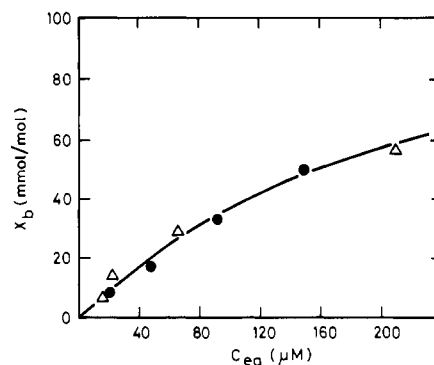


FIGURE 4: Comparison of SMS 201-995 binding to POPG/POPC (25/75 mol/mol) bilayers (Δ) and monolayers (●). The monolayers were compressed to 32 mN/m. If a surface area of  $A_p = 135 \text{ \AA}^2$  is used, the monolayer binding isotherm yields results identical with the bilayer binding isotherm. The theoretical curve was calculated with  $z_p = 1.3$ ,  $A_p = 135 \text{ \AA}^2$ , and  $K_p = 75 \pm 10 \text{ M}^{-1}$ , including  $\text{Na}^+$  binding with  $K_{\text{Na}} = 0.6 \text{ M}^{-1}$  (0.154 M NaCl, 10 mM Tris-HCl, pH 7.4).

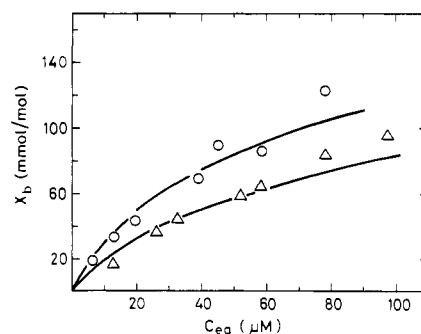


FIGURE 5: SMS 201-995 monolayer binding isotherms at 25 mN/m. The degree of binding was evaluated from the relative area increase by using a peptide surface area of  $A_p = 135 \text{ \AA}^2$ . (○) POPC/POPG (75/25 mol/mol) ( $K_p = 650 \text{ M}^{-1}$ ,  $z_p = 1.3$ ); (Δ) pure POPC ( $K_p = 2600 \text{ M}^{-1}$ ,  $z_p = 1.3$ ). The theoretical curves were calculated by using the Gouy-Chapman theory combined with a partition equilibrium, using the binding parameters given above (0.154 M NaCl, 10 mM Tris-HCl, pH 7.4).  $\text{Na}^+$  binding to PG is included with  $K_{\text{Na}} = 0.6 \text{ M}^{-1}$ .

The surface area of POPC and POPG can be estimated from monolayer measurements as  $A_L = 68 \text{ \AA}^2$  ( $73 \text{ \AA}^2$ ) at 32 mN/m (25 mN/m) (Evans et al., 1987). The peptide surface area,  $A_p$ , was determined as follows. Inspection of computer models of SMS 201-995 revealed a smooth surface area of about  $7 \times 20 = 140 \text{ \AA}^2$ . A value of  $120 \text{ \AA}^2$  was derived from measurements of the surface activity of peptide solutions, evaluating the Gibbs adsorption isotherm.<sup>3</sup> In the present analysis a value of  $A_p = 135 \text{ \AA}^2$  was used for the following reason. Several studies have demonstrated that the bilayer–monolayer equivalence pressure is about 32 mN/m; i.e., at this lateral pressure the lipid packing in a monolayer is similar to that in the bilayer [Schindler, 1979, 1980; Seelig, 1987; cf. also Demel et al. (1975) and Blume (1979)]. We have therefore measured the area increase of a POPC/POPG (75/25 mol/mol) monolayer at 32 mN/m as a function of the peptide concentration and, in parallel, have determined the bilayer binding isotherm under identical conditions. By use of eq 1, the monolayer binding isotherm was calculated for various values of  $A_p$ . Good agreement between the two data sets was obtained for  $A_p = 135 \text{ \AA}^2$  as is shown in Figure 4. Equation 1 corresponds to a linear scaling of  $\Delta A/A$  by a constant factor and the func-

<sup>3</sup> The measurement of the Gibbs adsorption isotherm of pure SMS 201-995 in solution and the determination of the peptide surface area by Dr. A. Seelig are gratefully acknowledged.

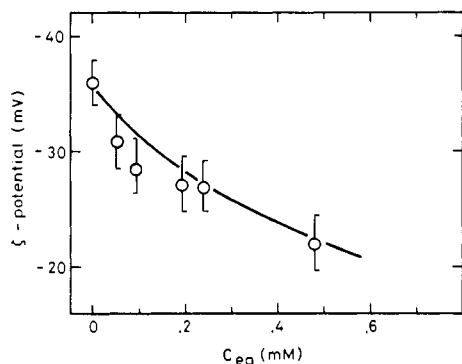


FIGURE 6:  $\zeta$ -Potential measurements of POPC/POPG (75/25 mol/mol) vesicles at various concentrations of SMS 201-995 peptide. The theoretical curve was calculated with  $K = 36 \text{ M}^{-1}$  and  $z_p = 1.3$ , including  $\text{Na}^+$  binding to PG with  $K_{\text{Na}} = 0.6 \text{ M}^{-1}$  (0.1 M NaCl, 10 mM Tris-HCl, pH 7.4).

tional form of the binding isotherm is thus identical for the monolayer and the bilayer.

Knowledge of the protein area,  $A_p$ , makes it possible to quantitatively analyze the binding isotherms at other lateral pressures. POPC and POPC/POPG (75/25) monolayers compressed at 25 mN/m are shown in Figure 5. At this pressure the lipid packing is soft enough to allow peptide penetration even into pure POPC monolayers. On the other hand, the binding of SMS 201-995 to the negatively charged mixed POPC/POPG monolayer is distinctly enhanced. A quantitative analysis (solid lines are theoretical curves) reveals that the increased binding to the mixed monolayer is a purely electrostatic effect and that, in fact, the chemical binding constant is larger for the pure POPC than for the mixed POPC/POPG monolayer (cf. below).

**$\zeta$ -Potential Measurements.** Multilamellar vesicles were formed by the method of Bangham et al. (1974) and the electrophoretic mobility measured in the stationary layer. The  $\zeta$ -potential,  $\zeta$ , was calculated from electrophoretic mobility,  $u$ , by using the Helmholtz-Smoluchowski equation

$$\zeta = (u\eta)/(\epsilon_r\epsilon_0) \quad (2)$$

where  $\eta$  is the viscosity of the aqueous phase,  $\epsilon_0$  is the permittivity of free space,  $\epsilon_r = 78$  is the dielectric constant of water (Aveyard & Haydon, 1973). Vesicles were incubated with varying concentrations of peptide; immediately after the  $\zeta$ -potential measurement, the vesicles were centrifuged and the free peptide concentration in the supernatant determined by UV spectroscopy. Figure 6 shows the effect of increasing peptide concentrations on the  $\zeta$ -potential of mixed POPC/POPG (75/25 mol/mol) multilamellar vesicles. The  $\zeta$ -potential decreases from  $-36.5 \text{ mV}$  in the absence of peptide to  $-22 \text{ mV}$  at  $0.5 \text{ mM}$  peptide concentration. The experimental conditions are identical with those of Figure 1 and the solid line was calculated with the same model and binding constant as used in Figure 1.

## DISCUSSION

**Analysis of the Binding Isotherm.** The analysis follows the approach described for melittin binding to charged lipid bilayers (Beschiaschvili & Seelig, 1990a). We include peptide penetration between lipids and  $\text{Na}^+$  binding to charged headgroups. The various steps are briefly summarized as follows.

The charged PG headgroups are assumed to be the only binding sites for  $\text{Na}^+$ ; no  $\text{Na}^+$  binding occurs at the PC headgroups [cf. Eisenberg et al. (1979) and Ermakov (1990)].  $\text{Na}^+$  binding follows a Langmuir adsorption isotherm and can be written as

$$X_{\text{Na}}/(1 - X_{\text{Na}}) = K_{\text{Na}}C_{\text{M,Na}} \quad (3)$$

$$X_{\text{Na}} = K_{\text{Na}}C_{\text{M,Na}}/(1 + K_{\text{Na}}C_{\text{M,Na}}) \quad (4)$$

$X_{\text{Na}}$  is the mole fraction of  $\text{Na}^+$  bound to phosphatidylglycerol

$$X_{\text{Na}} = n_{\text{PG,Na}}/n_{\text{PG}}^0 \quad (5)$$

$[n_{\text{PG}}^0 = \text{total amount of PG (moles)}; n_{\text{PG,Na}} = \text{number of PG molecules (moles) with } \text{Na}^+ \text{ bound}]$ .  $C_{\text{M,Na}}$  is the concentration of  $\text{Na}^+$  immediately above the plane of ion binding. If the membrane has a surface potential,  $\psi_0$ , the membrane-active surface concentration,  $C_{\text{M,Na}}$ , is related to the bulk equilibrium concentration,  $C_{\text{eq,Na}}$ , according to the Boltzmann distribution:

$$C_{\text{M,Na}} = C_{\text{eq,Na}} \exp(-\psi_0 F_0 / RT) \quad (6)$$

$F_0$  is the Faraday constant,  $R$  the gas constant, and  $T$  the absolute temperature. The  $\text{Na}^+$  binding constant is  $K_{\text{Na}} = 0.6 \text{ M}^{-1}$ . This value was determined from the  $\zeta$ -potential of mixed PC/PG vesicles in  $0.1 \text{ M NaCl} + 10 \text{ mM Tris-HCl}$  measured in the absence of peptide (Figure 6) and agrees with previous measurements (Eisenberg et al., 1979; Macdonald & Seelig, 1987; Ermakov, 1990). Knowledge of the surface potential,  $\psi_0$ , allows the calculation of  $X_{\text{Na}}$ .

If  $X_{\text{PG}}^0$  (moles of PG per mole of total lipid) denotes the mole fraction of PG in the membrane and  $z_p$  the effective charge of the peptide, then the surface charge density,  $\sigma$ , can be written as (Beschiaschvili & Seelig, 1990a)

$$\sigma = (e_0/A_L) \frac{-X_{\text{PG}}^0(1 - X_{\text{Na}}) + z_p X_b}{1 + (A_p/A_L)X_b} \quad (7)$$

where  $e_0$  is the elementary charge and  $X_b$  is the mole fraction of bound peptide per total lipid as defined above. The term  $(A_p/A_L)X_b$  corrects for protein penetration into the membrane. Since  $X_b$  is typically  $< 0.1$  and since  $A_p/A_L \approx 2$  in the present study, protein penetration introduces at most a 20% correction in the surface charge density. As described above,  $X_b$  can be determined experimentally via a centrifugation assay or via a monolayer expansion study. The unknowns in eq 7 are  $z_p$  and  $X_{\text{Na}}$ , where the latter, in turn, is a function of the surface potential  $\psi_0$ .

A second, independent relation between  $\sigma$  and  $\psi_0$  is given by the Gouy-Chapman equation [cf. Aveyard and Haydon (1973) and McLaughlin (1977, 1989)]

$$\sigma^2 = 2000\epsilon_0\epsilon_r RT \sum C_{i,\text{eq}} (e^{-z_i F_0 \psi_0 / RT} - 1) \quad (8)$$

where  $C_{i,\text{eq}}$  is the concentration of the  $i$ th electrolyte in the bulk aqueous phase (in moles per liter) and  $z_i$  is the signed valency of the  $i$ th species.

Combining the adsorption/binding equation (eq 7) with the Gouy-Chapman equation (eq 8), a self-consistent solution  $\psi_0$  can be found for each experimental value of  $X_b$ . The best fit to the experimental data was obtained with an effective peptide charge of  $z_p = 1.3$ , which is smaller than the formal charge of  $+2$ . The numerical data for  $\sigma$  and  $\psi_0$  are summarized in Table I. The negative surface potential  $\psi_0$  increases the peptide concentration toward the interface and the peptide concentration immediately above the plane of binding,  $C_{\text{M}}$ , is given by

$$C_{\text{M}} = C_{\text{eq}} \exp(-z_p F_0 \psi_0 / RT) \quad (9)$$

Numerical data for  $C_{\text{M}}$  are given in Table I. The last column of Table I then demonstrates that the ratio  $X_b/C_{\text{M}}$  remains approximately constant over the concentration range measured. The binding of SMS 201-995 to the mixed POPG/POPC

Table I: Binding of SMS 201-995 to POPC/POPG (75/25 mol/mol) and Pure POPC Coarse Liposomes<sup>a</sup>

| $C_{eq}$<br>( $\mu$ M)  | $X_b$<br>(mmol/mol) | $\sigma$<br>(mC/m <sup>2</sup> ) | $\psi_0$<br>(mV) | $\zeta$<br>(mV) | $C_M$<br>(mM) | $K_p$<br>(M <sup>-1</sup> ) |
|-------------------------|---------------------|----------------------------------|------------------|-----------------|---------------|-----------------------------|
| POPC/POPG, 0.1 M NaCl   |                     |                                  |                  |                 |               |                             |
| 60                      | 22                  | -35.6                            | -41.5            | -32.7           | 0.51          | 43                          |
| 96.5                    | 29                  | -33.8                            | -39.7            | -31.3           | 0.75          | 39                          |
| 140                     | 36                  | -32.1                            | -38.0            | -30.0           | 0.99          | 36                          |
| 175                     | 42.8                | -30.4                            | -36.2            | -28.7           | 1.13          | 38                          |
| 200                     | 42                  | -30.6                            | -36.5            | -28.9           | 1.31          | 32                          |
| 228                     | 49.5                | -28.8                            | -34.6            | -27.4           | 1.35          | 37                          |
| 260                     | 49                  | -28.9                            | -34.7            | -27.5           | 1.55          | 32                          |
| 310                     | 56                  | -27.2                            | -32.9            | -26.1           | 1.69          | 33                          |
| POPC/POPG, 0.154 M NaCl |                     |                                  |                  |                 |               |                             |
| 16                      | 7.3                 | -38.3                            | -37.3            | -28.05          | 0.11          | 67                          |
| 21                      | 14.8                | -36.3                            | -35.6            | -26.8           | 0.13          | 112                         |
| 65                      | 29                  | -32.7                            | -32.5            | -24.5           | 0.34          | 84                          |
| 210                     | 57                  | -25.7                            | -26.2            | -19.9           | 0.81          | 70                          |
| POPC, 0.154 M NaCl      |                     |                                  |                  |                 |               |                             |
| 270                     | 14                  | 4.17                             | 4.3              | 3.3             | 0.22          | 65                          |
| 180                     | 15.7                | 4.66                             | 4.8              | 3.7             | 0.14          | 111                         |
| 811                     | 42                  | 11.9                             | 12.3             | 9.4             | 0.43          | 66                          |

<sup>a</sup> 20 °C; 0.1 or 0.154 M NaCl, 10 mM Tris-HCl, pH 7.4.

membrane can thus be described by a simple surface partition equilibrium of the form

$$X_b = K_p C_M \quad (10)$$

with the partition constant  $K_p = 36 \pm 4 \text{ M}^{-1}$ . The solid line in Figure 1 represents the theoretical predictions of this Gouy-Chapman partition model.

The electrokinetic potential  $\zeta$  is the average electrostatic potential at the hydrodynamic plane of shear, which, for a 0.1 M 1:1 electrolyte solution, is assumed to be 0.2 nm above the membrane surface (Eisenberg et al., 1979). The variation of the electrostatic potential  $\psi(x)$  in the aqueous phase is also described by the Gouy-Chapman theory [cf. Aveyard and Haydon (1973) and McLaughlin (1989)] and by applying the standard formulas we have calculated the  $\zeta$ -potential using the Gouy-Chapman partition model and the experimental conditions of Figure 6. Good agreement between the experimental results and the predictions of the theory (solid line) was obtained.

The analysis of the  $\zeta$ -potential alone does not lead to a unique solution. Several parameter sets  $z_p$ ,  $K_p$  can provide a satisfying fit to the experimental results, e.g.,  $z_p = 2$ ,  $K = 10 \text{ M}^{-1}$  provides an almost equally good agreement between experiment and theory as the parameter set chosen in Figure 6. Likewise, the interpretation of the binding isotherm (Figure 1) allows some variation in  $z_p$  and  $K_p$ , however, within narrower limits than the  $\zeta$ -potential measurements. On the other hand, taking the two experiments together  $z_p = 1.3$  and  $K_p = 36 \pm 4 \text{ M}^{-1}$  are the only possible parameters that fit both curves simultaneously.

**Molecular Model of Peptide-Lipid Interaction.** From inspection of molecular models the approximate dimensions of SMS 201-995 are deduced as  $7 \times 7 \times 20 \text{ \AA}^3$ . Experimentally, the monolayer studies lead to a surface area requirement of

$135 \text{ \AA}^2$ , which suggests that the peptide enters monolayers and bilayers with one of its large faces ( $7 \times 20 \text{ \AA}^2$ ) parallel to the membrane surface. Such an alignment excludes the penetration of the peptide into the hydrocarbon core of the membrane, a conclusion that is also supported by fluorescence measurements. The maximum of the tryptophan fluorescence emission spectrum shifts from 351 nm in water to 339 nm upon lipid binding, indicating a dielectric constant of  $\epsilon \sim 7$  for the membrane environment of the tryptophan residue (Beschi-schvili & Seelig, 1990b). This result suggests that the tryptophan side chain is located in the inner part of the headgroup layer but not in the hydrocarbon layer ( $\epsilon \sim 2$ ).

The partition constant  $K_p = 36 \text{ M}^{-1}$  for SMS 201-995 is small and indicates only a weak binding to neutral membrane surfaces. For negatively charged membranes the binding/partitioning is, however, enhanced due to electrostatic attractions; depending on the charge density of the membrane surface, the amount of bound peptide can increase by more than a factor of 10 compared to neutral membranes.

If  $\text{Na}^+$  binding and electrostatic attraction are ignored (as is quite common in peptide binding studies), the data of Table I can be evaluated in terms of a conventional Scatchard plot

$$X_b/C_{eq} = K_{app}(1 - nX_b) \quad (11)$$

The apparent binding constant,  $K_{app}$ , is related to the partition coefficient  $K_p$  defined above

$$K_{app} \sim K_p(C_M/C_{eq}) \quad (12)$$

The Scatchard analysis of Table I (0.1 M NaCl) yields an approximately straight line (correlation coefficient  $>0.9$ ) with  $K_{app} \approx 460 \text{ M}^{-1}$  and  $n = 11.5$ . In a naive view, this result could be interpreted as a specific binding of the peptide to the negatively charged lipids with 11–12 lipids constituting a peptide binding site. While empirically satisfying, the Scatchard analysis provides a physically unrealistic picture of peptide binding. The shortcomings of the Scatchard analysis for the problem at hand have been discussed elsewhere (Seelig & Macdonald, 1989; Seelig, 1990).

Table II summarizes the binding/partitioning data of the various systems studied. Increasing the salt concentration from 0.1 M NaCl to 0.154 M NaCl increases  $K_p$  by a factor of 2 to  $K_p = 75 \text{ M}^{-1}$  as deduced from the POPC/POPG bilayer binding data of Figure 4. A similar salt effect was observed for the binding of melittin to different types of lipid bilayers (Stankowski & Schwarz, 1990). These results could be explained by the well-known "salting out" of nonpolar substances since the addition of salt usually decreases the solubility of nonpolar substances in water. Measurements on peptide solubility in water at different salt concentrations could shed further light on this problem. We have also measured SMS 201-995 binding to neutral POPC bilayers at 0.154 M NaCl. Relatively large peptide concentrations must be employed in the centrifugation assay in order to detect measurable binding effects, which eventually also lead to aggregation of peptide. Table I thus includes only binding data obtained at  $C_{eq} < 1 \text{ mM}$ . The data were evaluated by the same model as described

Table II: Summary of Binding Parameters

| system    | comp (mol/mol)    | [NaCl] <sup>a</sup><br>(M) | pressure<br>(mN/m) | lipid area<br>( $\text{\AA}^2$ ) | peptide area<br>( $\text{\AA}^2$ ) | peptide<br>charge | $K_p$ (M <sup>-1</sup> )    |
|-----------|-------------------|----------------------------|--------------------|----------------------------------|------------------------------------|-------------------|-----------------------------|
| bilayer   | POPC/POPG (75/25) | 0.10                       |                    | 68                               | 135                                | 1.3               | $36 \pm 4$                  |
| bilayer   | POPC/POPG (75/25) | 0.154                      |                    | 68                               | 135                                | 1.3               | $75 \pm 10$                 |
| monolayer | POPC/POPG (75/25) | 0.154                      | 32                 | 68                               | 135                                | 1.3               | $75 \pm 10$                 |
| monolayer | POPC/POPG (75/25) | 0.154                      | 25                 | 73                               | 135                                | 1.3               | $632 \pm 160$               |
| monolayer | POPC (100)        | 0.154                      | 25                 | 73                               | 135                                | 1.3               | $(2.5 \pm 0.6) \times 10^3$ |

<sup>a</sup> Plus 10 mM Tris-HCl, pH 7.4.

above, yielding  $K_p \approx 80 \text{ M}^{-1}$ , in excellent agreement with the analysis of the charged membrane.

Decreasing the lipid packing density via the lateral pressure facilitates the penetration of the peptide into the lipid monolayers:  $K_p$  increases from 75 to  $630 \text{ M}^{-1}$  as the monolayer pressure is reduced from 32 to 25 mN/m for the mixed POPG/POPC monolayer. The binding constant at 25 mN/m increases even further when the membrane composition is changed to pure POPC, i.e., at this lower pressure the peptide penetration is no longer described by a common binding constant but becomes dependent on the lipid composition. The molecular origin of this effect could be a variation in the molecular area or a change in the dissociation state of POPG with lateral pressure.

For comparison, the binding of somatostatin to mixed POPC/POPG (75/25) lipids was also measured by using the monolayer technique. The partition constant was estimated as  $920 \text{ M}^{-1}$  (at 32 mN/m; 0.154 NaCl) and the effective peptide charge was  $z_p = 1.6$ . Somatostatin has approximately twice the molecular weight of SMS 201-995 and the larger binding constant reflects an increase in hydrophobicity of somatostatin.

The SMS 201-995 partition constant of  $36 \text{ M}^{-1}$  corresponds to a free energy  $\Delta G = -RT \ln 55.5 K_p = -4.5 \text{ kcal/mol}$ . Since the loss of one rotational and two translational degrees of freedom upon membrane binding requires  $\sim 10 \text{ kcal/mol}$  [cf. Janin and Chotia (1978)], the total free energy change is about  $-14.5 \text{ kcal/mol}$ . If this energy is provided by the hydrophobic effect and if the transfer of  $1 \text{ \AA}^2$  of nonpolar surface yields a free energy of  $-20 \text{ cal}$  (Chotia, 1974; Richards, 1977), the total buried surface area is about  $725 \text{ \AA}^2$ , i.e., approximately 60–70% of the total peptide surface area.

The effective charge of SMS 201-995 in the present binding studies was  $z_p = 1.3$ , which is smaller than the formal charge of +2. Such discrepancies have been noted previously in binding studies of substance P (Seelig & Macdonald, 1989) and, even more pronounced, of melittin (Schwarz & Beschiaschvili, 1989; Kuchinka & Seelig, 1989; Beschiaschvili & Seelig, 1990). Explanations for these differences could be pK shifts upon membrane binding, discrete charge effects, or the influence of large charge separations [cf. McLaughlin (1989)].

**Conclusions.** Most biological membranes carry a negative surface charge since the typical lipid composition is 80% neutral lipids and 20% negatively charged lipids. The effect of this surface charge is to attract ligands of opposite charge and to repel those of like charge. The associated surface potential may differ from membrane to membrane and may also vary with the cellular environment. In order to obtain comparable data for the binding of a charged peptide, potential-induced concentration variations must be corrected for. In the present analysis, the use of peptide interfacial concentrations instead of bulk concentrations led to a consistent interpretation of different types of measurements and to a single partition model for peptide binding. The ambiguities in the molecular interpretation could be greatly reduced by measuring both the binding isotherm and the electrokinetic potential.

**Registry No.** POPC, 26853-31-6; POPG, 81490-05-3; SMS 201-995, 83150-76-9; NaCl, 7647-14-5.

## REFERENCES

Aveyard, R., & Haydon, D. A. (1973) *An introduction to the principles of surface chemistry*, Cambridge University Press, Cambridge.

- Bangham, A. D., Hill, M. W., & Miller, N. G. A. (1974) *Methods Membr. Biol.* 1, 1–68.
- Beschiaschvili, G., & Seelig, J. (1990a) *Biochemistry* 29, 52–58.
- Beschiaschvili, G., & Seelig, J. (1990b) *Biochim. Biophys. Acta* (in press).
- Blume, A. (1979) *Biochim. Biophys. Acta* 557, 32–34.
- Chotia, C. (1974) *Nature* 248, 338–339.
- Demel, R. A., Geurts van Kessel, W. S. M., Zwaal, R. F. A., Roelofs, B., & van Deenen, L. L. M. (1975) *Biochim. Biophys. Acta* 406, 97–107.
- Eisenberg, M., Gresalfi, T., Riccio, T., & McLaughlin, S. (1979) *Biochemistry* 18, 5213–5223.
- Engelman, D. M., Steitz, T. A., & Goldman, A. (1986) *Annu. Rev. Biophys. Biophys. Chem.* 15, 321–353.
- Ermakov, Y. A. (1990) *Biochim. Biophys. Acta* 1023, 91–97.
- Evans, R. W., Williams, M. A., & Tinoco, J. (1987) *Biochem. J.* 245, 455–462.
- Fromherz, P. (1975) *Rev. Sci. Instrum.* 46, 1380–1385.
- Holladay, L. A., Rivier, J., & Puett, D. (1977) *Biochemistry* 16, 4895–4900.
- Jacobs, R. E., & White, S. H. (1986) *Biochemistry* 25, 2605–2612.
- Jacobs, R. E., & White, S. H. (1989) *Biochemistry* 28, 3421–3437.
- Jain, M. K., Rogers, J., Simpson, L., & Gierach, L. M. (1985) *Biochim. Biophys. Acta* 816, 153–162.
- Janin, J., & Chotia, C. (1978) *Biochemistry* 17, 2943–2948.
- Kuchinka, E., & Seelig, J. (1989) *Biochemistry* 28, 4216–4221.
- Lee, S., Yoshida, M., Mihara, H., Aoyagi, H., Kato, T., & Yamasaki, N. (1989) *Biochim. Biophys. Acta* 984, 174–182.
- Macdonald, P. M., & Seelig, J. (1987) *Biochemistry* 26, 1231–1240.
- Maurer, R., Gaehwiler, B. H., Buescher, H. H., Hill, R. C., & Roemer, D. (1982) *Proc. Natl. Acad. Sci. U.S.A.* 79, 4815–4817.
- McLaughlin, S. A. (1977) *Curr. Top. Membr. Transp.* 9, 71–144.
- McLaughlin, S. (1989) *Annu. Rev. Biophys. Biophys. Chem.* 18, 113–136.
- Nozaki, Y., & Tanford, C. (1971) *J. Biol. Chem.* 246, 2211–2217.
- Richards, F. (1977) *Annu. Rev. Biophys. Bioeng.* 6, 151–176.
- Schindler, H. (1979) *Biochim. Biophys. Acta* 555, 316–336.
- Schindler, H. (1980) *FEBS Lett.* 122, 77–79.
- Schwarz, G., & Beschiaschvili, G. (1989) *Biochim. Biophys. Acta* 979, 82–90.
- Seelig, A. (1987) *Biochim. Biophys. Acta* 899, 196–204.
- Seelig, A., & Macdonald, P. M. (1989) *Biochemistry* 28, 2490–2496.
- Seelig, J. (1990) *Cell. Biol. Rep.* 14, 353–360.
- Stankowski, S., & Schwarz, G. (1990) *Biochim. Biophys. Acta* 1025, 164–172.
- Surewicz, W. K., & Epand, R. M. (1984) *Biochemistry* 23, 6072–6077.
- Surewicz, W. K., & Epand, R. M. (1985) *Biochemistry* 24, 3135–3144.
- Surewicz, W. K., & Epand, R. M. (1986) *Biochim. Biophys. Acta* 856, 290–300.
- Tamm, L. K., & Seelig, J. (1983) *Biochemistry* 22, 1474–1483.
- Toner, M., Vaio, G., McLaughlin, A., & McLaughlin, S. (1988) *Biochemistry* 27, 7435–7443.